Performance-Based Seismic Design of a Large Seismically Isolated Structure: Istanbul Sabiha Gökçen International Airport Terminal Building

Atila Zekioglu, Huseyin Darama, Baris Erkus
Arup North America Ltd.
Los Angeles, California

Abstract

This paper describes the performance-based seismic design of the Sabiha Gökçen[1] International Airport (SGIA) Terminal Building in Istanbul, Turkey utilizing seismic-isolation concept with triple-friction-pendulum devices. When completed, the SGIA terminal building will be one of the largest seismically isolated structures in the world with an area over 160,000 square meters and 252 seismic isolators. Achieving explicit seismic performance was part of the client's design requirements to protect their investment, as they perceive earthquakes to be the biggest risk to their business. Arup, through the use of performance-based seismic design, facilitated the discussions with the client and established the following seismic performance objectives: (1) Operational Level for a Design Basis Earthquake (DBE), (2) Structural Immediate Occupancy Level for a Maximum Considered Earthquake (MCE). To achieve these objectives, Arup evaluated various seismic protection systems with the client, and a base-isolation system with triple-friction pendulum devices was selected for its performance and cost-effective properties. A site specific Probabilistic Seismic Hazard Assessment (PSHA) was conducted to develop the DBE and MCE response spectra curves and spectrally matched time history pairs. Next generation attenuation relationships and multiple scenarios of fault rupture/directivity were included in the PSHA study. The structural system was analyzed using equivalent static, linear dynamic and time history procedures, including a "beyond the code requirement" investigation of the structural members at MCE hazard with FEMA recommended acceptance criteria per the selected performance objectives. A comparative study was performed showing the effectiveness of the current code based analysis and design procedures. Overall, the seismically isolated structure met and surpassed the performance objectives while achieving an 80% reduction in the base shear, and a significant decrease in the story drift and floor accelerations.

[1] Sabiha Gökçen (1913-2001) was the first female pilot from Turkey and the first female combat pilot in the world.

Project Description

Sabiha Gökçen International Airport (SGIA) is one of the two major airports serving Istanbul, the largest city in Turkey with a population exceeding 11 million. Located about 30 miles northeast of central Istanbul (Figure 1), SGIA has currently an annual passenger capacity of 5 million. Planned in the early 1990s and constructed in 2001, SGIA was aimed not only to address the future air traffic needs of Istanbul, but also to provide logistic support to a local high technology investment park. Since then, the number of passengers served has increased tremendously; an 80% annual average increase between the years of 2002 and 2007 has been reported.

Figure 1. Location of SGIA

In 2006, the Turkish government decided to increase the capacity of SGIA through the addition of a new international terminal with various other surrounding facilities. In July 2007, a bid was held for a concession with a build-operate-transfer model, where the winner buys the operation rights of SGIA for 20 years for €1.93 billion and agrees to increase the total annual capacity to 15 million passengers by building a new terminal with a minimum €250 million investment.

Istanbul Sabiha Gökçen International Airport Investment Development and Operations Inc. (abbreviated as ISGIDO in this paper), a multi-national consortium formed by Limak Holdings, GMR Infrastructure and Malaysia Airports Holdings Berhad, won the bidding, signed the agreement in March 2008 and started the new terminal construction immediately after the groundbreaking ceremony held in May 2008.

The new terminal and its facilities are being constructed on a total area of 320,000 square meters. The project constitutes a new 160,000 square meters integrated domestic and international terminal building, a parking structure, a hotel, a new VIP terminal and various other airport facilities (GMR, 2008). The terminal is expected to be operational by the end of 2009 (Figure 2).

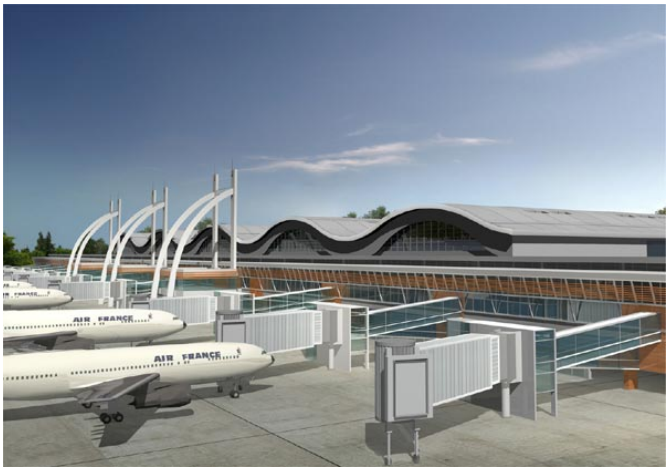

Figure 2. Design concept image of the New Sabiha Gökçen International Terminal Building (courtesy Tekeli-Sisa Architects)

Performance Objectives and Scope of Work

It is well known that the Istanbul region is seismically active and experiences large earthquakes periodically due to active faults located very close to the city (Figure 3). The tragic 1999 Kocaeli earthquake killed 17,000, injured 43,000 and forced 250,000 people to relocate (USGS, 2000). The estimates of property losses range from $3 to $6.5 billion, not to mention the overall economic loss to the country as the earthquake hit a heavily industrialized area of Turkey.

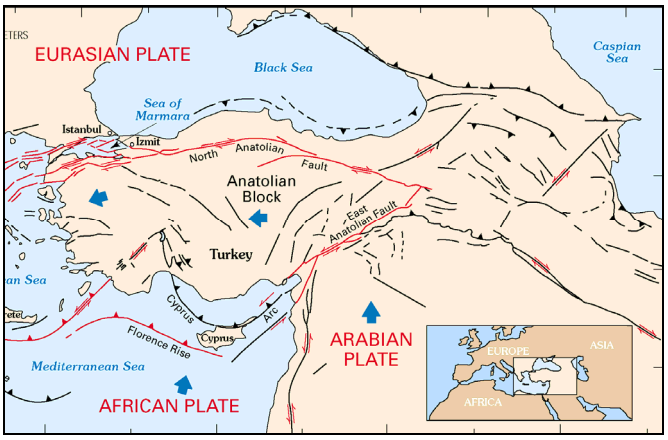

Figure 3. The tectonic map of Turkey (USGS, 2000)

The clear earthquake potential of the SGIA location has raised the seismic performance of the airport facility to the highest priority for ISGIDO, not only to protect their investments, but also to keep this crucial infrastructure operational (for emergency transportation) after a major earthquake. Particularly, the new terminal building is required to have a well defined seismic performance by the client as it is the most important part of the project. Arup initiated a performance-based design framework with the client and defined the following two major seismic performance level objectives based on the client's requirements for the terminal building:

1. The building will be designed for Operational Level *i.e.*, no structural and no non-structural damage for an earthquake hazard with a uniform 10% probability of exceedance in 50 years, which is equivalent to a hazard with a return period of 475 years. This earthquake hazard is commonly known as Design Basis Earthquake (DBE) or design earthquake in practice.
2. The building will be designed for Structural Immediate Occupancy for an earthquake hazard with a uniform 2% probability of exceedance in 50 years, which is equivalent to a hazard with a return period of 2,475 years. This earthquake hazard is known as Maximum Considered Earthquake (MCE).

As ISGIDO understood that the design of a standard fixed-based structure that will satisfy the stringent seismic performance objectives listed above will be uneconomical and infeasible, they decided to implement a base-isolation system. A seismic base isolation system with energy dissipation capabilities enables shifting/elongation of the fundamental periods of structure and provides a significant increase in the effective damping. These two key features provide a significant reduction in the seismic design forces and inter-story drifts of the superstructure, and hence reduce the risk of structural and non-structural earthquake damage. Arup's structural scope of work has been defined as acting as an advisor to the client in the selection of isolation devices (providing evaluations of the proposals received from various isolation device manufacturers) and providing the performance-based design of the overall base-isolated steel structure.

A project team, based in Istanbul and Los Angeles, was formed and the following key deadlines were established during the kickoff meeting with the client in March 2008:

- Mid-April, 2008: Foundation design.
- End of April, 2008: Evaluation of four seismic isolation bearing systems. These included a double-friction-pendulum device, a triple-friction-pendulum device, a lead-rubber bearing and a high-damping rubber bearing.
- Mid-May, 2008: Selection and purchase order of seismic isolation bearings.

At present, the Turkish seismic code for buildings, TEC 98/07 has neither a guideline for performance-based design of structures nor requirements for analysis and design of seismically isolated buildings. Therefore, ASCE 7-05 was selected for the basis of performance-based design of the base isolated terminal building. The determination of the isolator bearing displacement demand is essential in the sizing of isolators and directly impacts the cost of the bearings. Selection of the fundamental period of isolation bearings and the site-specific seismic hazard are the two key inputs influencing the displacement demand. The calculation of bearing displacements is an iterative procedure for static and response spectrum analysis as effective stiffness and effective damping properties of seismic isolators are dependent on the displacement. A more reliable approach is the determination of the displacement response histories by conducting non-linear time-history analyses for multiple earthquake scenarios for DBE and MCE hazards.

In March 2008, there was no Probabilistic Site Specific Hazard analysis (PSHA) available that could be used for the evaluation of the isolators. In order to meet the client's stringent construction and procurement schedule, Arup's design team started isolation system evaluations using static and dynamic response spectrum analyses on the basis of a suite of modified response spectra from multiple American codes (ASCE 7-05, IBC 2006 and etc.) and the Turkish seismic code (TEC 98/07). These studies showed that the triple-friction-pendulum isolation bearings by Earthquake Protection Systems, Inc. (EPS) met the performance and cost requirements of the client and, hence, they were selected as the isolator devices for the SGIA project. Triple-friction-pendulum bearings have been extensively investigated and are shown to be effective for seismic protection of structures (Fenz and Constantinou, 2008a and 2008b). In the later stages of the project, the selection of the isolator was further investigated and verified through detailed response spectrum and non-linear time-history analyses as the PSHA became available.

This paper presents the performance-based design of the base-isolated SGIA terminal building. First, the site-specific PSHA is explained, and the DBE and MCE hazards are defined. Second, the superstructure system and computer modeling of the building are explained. Then, the design and modeling of the triple-friction-pendulum is given. Fourth, the analysis procedures used in the performance analysis are explained. Finally, the structural performance is investigated and tabular and graphical results are presented.

Review of the Code Provisions and Seismic Hazard

In this section, a review of the DBE and MCE response spectrum curves used the analysis and design of the base isolation and superstructure of the SGIA building are given. First, a brief review of Turkish and American seismic hazard definitions is given. Then, the site-specific PSHA study is explained and the resulting response spectrum curves are compared to the code-based response spectrum curves.

a) Turkish Code, TEC 98/07:

In the Turkish seismic code, the basis for determination of seismic loads is the spectral acceleration coefficient, $A(T)$, which is given by

$$A(T) = A_o\, I\, S(T) \tag{1}$$

where A_o is the effective ground acceleration coefficient, I is the importance factor, and $S(T)$ is the spectrum coefficient, which is a function of the local site conditions and building natural period, T. $S(T)$ is given by

$$\begin{aligned} S(T) &= 1 + 1.5\frac{T}{T_A} && (0 \le T \le T_A) \\ S(T) &= 2.5 && (T_A \le T \le T_B) \\ S(T) &= 2.5 + \left(\frac{T_B}{T}\right)^{0.8} && (T_B \le T) \end{aligned} \tag{2}$$

where T_A and T_B are the spectrum characteristic periods.

Seismic zones are classified as 1, 2, 3 and 4; 1 being the most severe seismic zone. Also, a local site class, Z1, Z2, Z3 or Z4 is assigned to the building based on the soil condition. The parameter A_o depends on the seismic zone and provided by a table in the code. Similarly, T_A and T_B depend on the local site class and are provided by a table in the code. The seismic base shear, V_t is given by

$$V_t = \frac{W \cdot A(T_1)}{R_a(T_1)} \geq 0.10 A_o \cdot I \cdot W \quad (3)$$

where W is the seismic weight of the structure, R_a is the seismic load reduction factor, and T_1 is the first natural vibration period of the structure, which can be found by code defined equation similar to ASCE 7-05 period calculations or a computer based analysis. R_a is further defined as

$$R_a(T) = 1.5 + (R - 1.5)\frac{T}{T_A} \qquad (0 \leq T \leq T_A)$$
$$R_a(T) = R \qquad (T_A < T) \quad (4)$$

According to Turkish code,

$$W = \sum DL + 0.6 \sum LL \quad (5)$$

where R is the structural behavior factor.

A brief base shear calculation according to TEC 98/07 is given as follows. For a building located at Seismic Zone 1 (DBE Hazard) and resting on a soil type Z2 (NEHRP class C), seismic forces can be calculated as follows (A_o=0.4 for Zone-1, I = 1, T_A = 0.15, T_B = 0.40 for Soil Type Z2, T1 = 3.0 sec. Presented for R=8, per ASCE 17.5.4.3, and R=2.0, per ASCE 17.5.4.2, as there is no requirement in TEC-98/07 for seismically isolated structures)

$$S(3) = 2.5\left(\frac{0.4}{3}\right)^{0.8} = 0.499$$
$$R_a(3) = \min(R_{\text{fixed\_base}} \times 3/8,\ 2) = 2 \quad (6)$$

$$V_t = 0.10W > V_{\min} = 0.10\, A_o\, I\, W = 0.04W \quad (7)$$

b) Uniform Hazard Response Spectra (NEHRP/IBC-2006/ASCE 7-05):

The design response spectra in the recent American codes is well-documented (NEHRP 2003, ASCE 7-05, and IBC 2006) and is briefly reviewed herein.

The first step in defining the design response spectrum is to find the mapped accelerations parameters, S_s (0.2 sec acceleration parameter) and S_1 (1 sec acceleration parameter), which are provided by the soils report (Belirti, 2008). These parameters are then multiplied with the site coefficients, F_a and F_v to consider the site effects, which define the MCE response spectrum parameters. The design spectral acceleration parameters are found multiplying the MCE parameters by (2/3). The geophysical investigations conducted by Belirti (2008) revealed that the site corresponds to Class C. A summary of the response spectrum parameters is given in Table 1.

Table 1. NEHRP spectrum parameters (Site Class C)

Parameter	DBE	MCE
S_S (m/sec^2)	8.397	12.812
S_1 (m/sec^2)	3.963	6.151
T_0 (sec)	0.123	0.125
T_S (sec)	0.614	0.624
F_a	1.0	1.0
F_v	1.3	1.3
T_L (sec)	8	8

c) Attenuation based Site Specific Response Spectra curves including directivity effects

A site specific PSHA was conducted by Erdik *et al*. (2008) to evaluate seismicity of the SGIA site and provide design seismic hazard for the DBE and MCE events.

The North Anatolian Fault (Figure 3) has two major branches that are the closest faults to the SGIA terminal building site. These are the Northern Boundary Fault (NBF) and Central Marmara Fault (CMF), which are around 20 km and 50 km away from the building site, respectively. The NBF and CMF were used as the basis of the hazard study by Erdik *et al*. (2008). The length of the NBF is about 36 km and located in the East-West direction. The CMF is approximately 108 km long and located on the west of NBF in the North-South direction. Erdik *et al*. (2008) used the "latest attenuation relationships provided by Campbell and Bozorgnia (2008) for the random and the average horizontal component and by the attenuation relationship of Boore and Atkinson (2008) for the average horizontal component and for V_s = 500 cm/sec."

It is argued that "the attenuation based spectra would be physically better suited and more rational for the generation of spectrum compatible time histories compared to the code-based spectral shapes" (Erdik *et al*., 2008). Further it is recommended that directivity effects should be included in the study since the site is at a critical location where the directivity effects will increase the ground motion levels due to the unruptured fault segments (Erdik *et al*., 2008).

It is found that the directivity effects will increase the ground acceleration by 20% for a structural period of 2.5 sec, which is "caused by the eastward rupture scenario associated with the NBF" (Erdik *et al*., 2008). It is also noted that a similar increase will be found if the method given by Somerville *et al*. (1997) is used for a site located in the front directivity region

and in direction of the fault strike (X cos $\theta = 0.63$)" (Erdik *et al*., 2008) (see Figure 4).

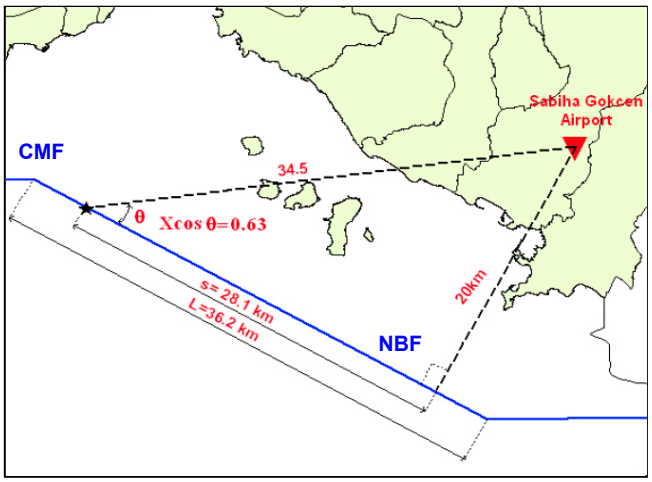

Figure 4. The site and causative fault configuration (Erdik *et al*., 2008)

The MCE level response spectrum obtained from the attenuation model given by Campbell and Bozorgnia (2008) with following parameters

- M = 7.25
- R = 20 km
- V_s = 500 km/s
- Strike slip type fault
- Vertically dipping fault plane
- Random horizontal component
- Epsilon = 2.1
- 2% exceedance probability

is increased by 20% for long periods and presented in Figure 4. This spectrum is also used as the basis of time-domain ground motion simulation. Comparison of the site-spectrum hazard to the code-based spectrum is given in Figures 5 and 6.

For time-history analysis, seven ground motion records from three earthquakes are selected such that selected earthquake locations have seismological characteristics similar to the SGIA site. These are 1992 Mw=7.3 Landers, 1999 Mw=7.4 Kocaeli, and 1979 Mw=6.5 Imperial Valley earthquakes. The selected ground motion time histories are modified to match the amplified MCE and DBE response spectra, where the ASCE 7-05 requirements are satisfied *i.e.*, "the square root of sum of squares (SRSS) spectrum of each record is not less than 90% of the amplified spectrum multiplied by 1.3 in the period range of interest, which is 1.25 sec to 3.5 sec" (Erdik *et al*., 2008) (see Figure 7). The MCE and DBE response spectrums and the ground acceleration time-histories provided by the site-specific PSHA study are used in the analysis and design of the SGIA building.

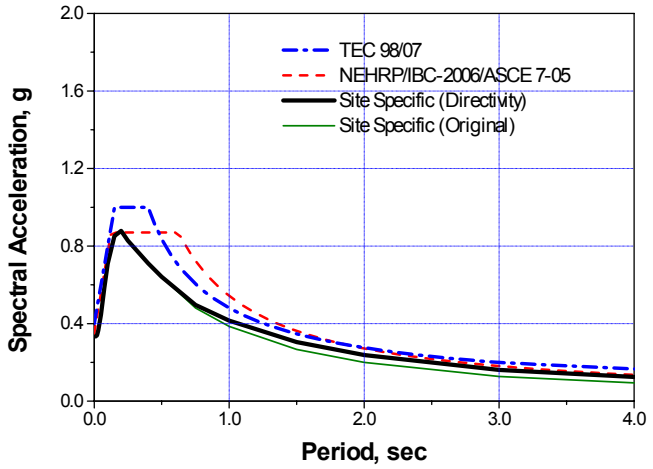

Figure 5. Code specified vs. Site Specific Response Spectra curves (DBE event) for 5% damping

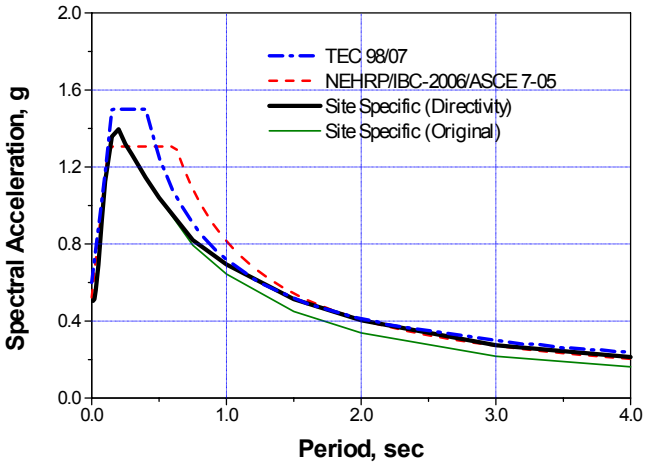

Figure 6. Code specified vs. Site Specific Response Spectra curves (MCE event) for 5% damping

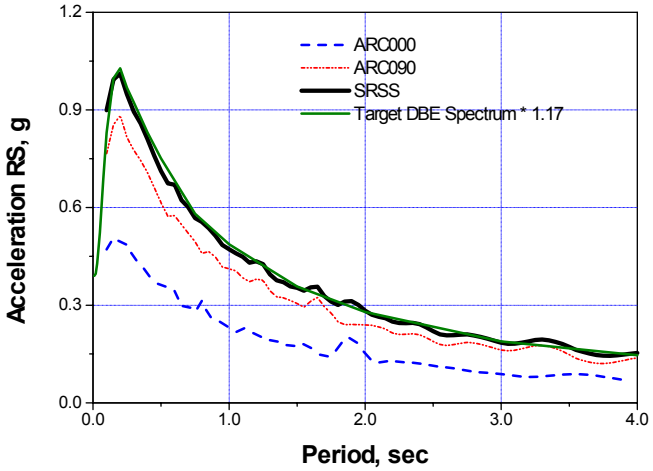

Figure 7. Spectrum matching by ASCE 7-05 criteria, ARC000/090 from 1999 Mw=7.4 Kocaeli (MCE)

Structural System Description and Modeling

The new SGIA Terminal building is a steel structure with a plan dimension of 160 meters by 272 meters. The total building height is approximately 32.5 meters. The building consists of 4 stories above and a basement floor below the isolation plane. Typical floor heights are 6 meters at the ground floor and 5 meters at the upper levels. The total floor area is more than 160,000 square meters.

The gravity system of the superstructure is composed of concrete filled steel decks, composite steel beams and composite steel columns. The clear span length supported by the columns is 16 meters in both directions. The framing for the stairs and elevators below the isolation plane is suspended from and braced by the isolated super structure above.

The roof system consists of light steel space purlin systems running longitudinally and located at every 8 meters and braced in the transverse direction. The purlin has a parabolic curve form with a depth of 12 meters and 6 meters placed evenly next to each other. They are pin-supported by the top of the columns at every 32 and 48 meters. Building roof plan and a longitudinal section showing building elevation are shown in Figure 8. A typical roof truss system and truss-column connection detail is shown in Figure 9.

The superstructure resists lateral loads by a system of steel moment frames through rigid horizontal diaphragms. The isolators are supported by the cantilevered concrete columns, which are supported by the foundations. There are 252 triple-friction-pendulum isolators that are distributed over the entire plan. The concrete compressive strength is selected to be 35 MPa, and the structural steel has yield strength of 355 MPa.

A three-dimensional computer model of the SGIA building is generated in the finite element analysis package, SAP2000 Version 11. The geometry and dimensions of the building as well as the initial sizes of the structural elements are provided by the architect. There are several assumptions and simplifications implemented in the SAP2000 model. First of all, the complex roof system is represented as an equivalent mass in the model since inclusion of this part of the structure in the model will not have a significant impact on the overall seismic behavior and design. Rather, the roof is analyzed separately for the seismic forces derived from the building model. Also, the slabs are modeled as part of the composite beams instead of using shell elements to improve the time-efficiency of the analysis. The slabs are modeled as rigid and code required accidental torsion is included, which is further explained in the following sections.

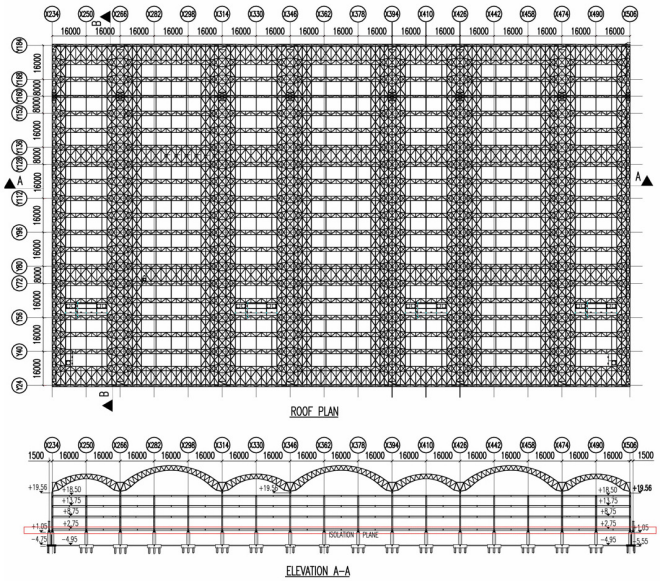

Figure 8. Building roof plan and elevation

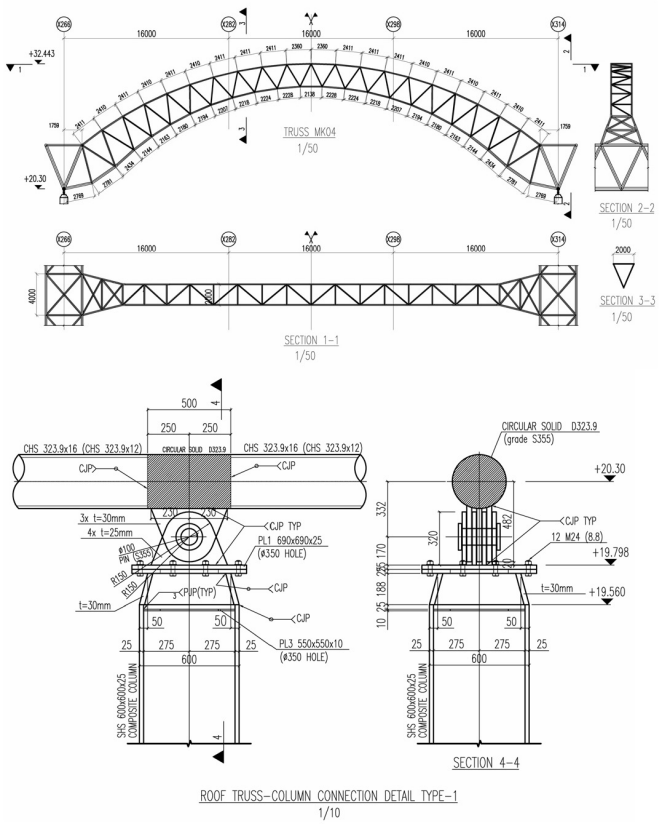

Figure 9. Typical roof truss and connection detail

Isolator Bearing Design

In general, isolator design is an iterative procedure, where the structural performance determines the isolator parameters, which in turn affect the overall structural performance. The first step in the design of friction-pendulum isolator is to find the maximum displacement that the isolators will experience as it is the most important parameter that will determine the dimensions of the isolator. The isolator displacements are mainly effected by three parameters: target isolated building period T_{eff}, axial load on the isolators W, and the level of the earthquake excitation.

It is recommended that the target isolated building period T_{eff}, is selected such that

$$T_{\text{eff}} \geq 3 \times T_{\text{o}} \tag{8}$$

where T_{o} is the period of the fixed-base structure.

Stiffness and period of friction pendulum devices depend on the curvature radius of the concave surface R, of the dish and is given by

$$T = 2\pi\sqrt{R/g} \tag{9}$$

Further, the effective stiffness K_{eff}, and effective damping β_{eff}, parameters of the device are given by

$$K_{\text{eff}} = \frac{W}{R} + \frac{uW}{D} \tag{10}$$

$$\beta_{\text{eff}} = \frac{2}{\pi}\frac{u}{u + (D/R)} \tag{11}$$

where D is the isolator displacement and u is the friction coefficient.

The superstructure has a fixed base period of 0.8 seconds. Average vertical load on isolators is approximately 5350 kN. The triple-friction-pendulum bearing (by EPS), with a theoretical period of 3 seconds and displacement limit of 345 mm, is selected on the basis of performance and cost. The effective damping provided by the isolators is 38% and 30% at DBE and MCE events respectively.

Prototype and production tests started in late May 2008 at EPS's facility at Mare Island in California upon the issue of the purchase order by the client (Figure 10). An idealized nonlinear shear-displacement curve obtained from the tests is used in the modeling of triple-friction-pendulum isolators (Figure 11). Geometry of the proposed bearings is shown in Figure 12 (Zayas *et al*. 2008a, 2008b and 2008c).

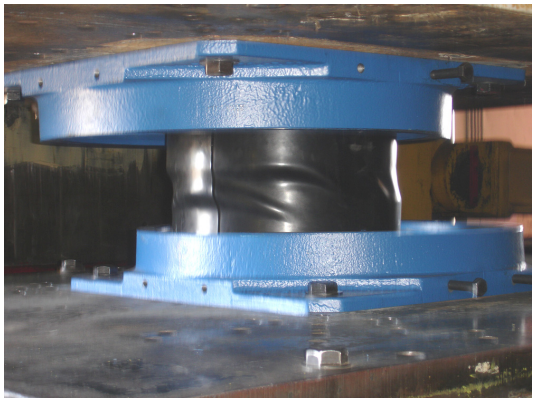

Figure 10. Real-time prototype test performed by EPS (model FPT4600)

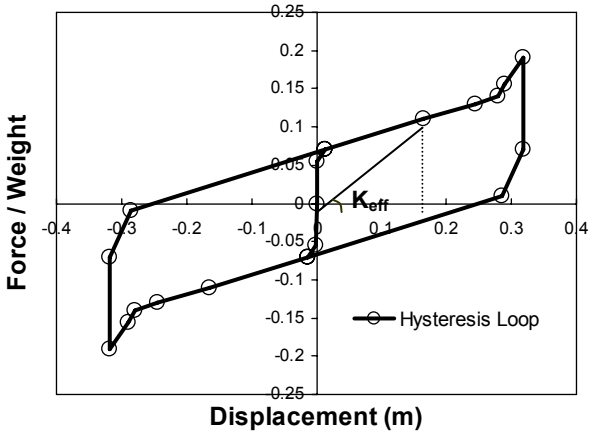

Figure 11. Idealized nonlinear hysteresis model curve for the triple-friction-pendulum isolator

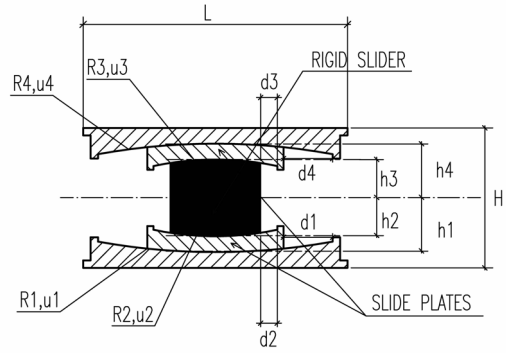

R1	88"
R2	16"
R3	16"
R4	88"

d1	5.7"
d2	2.25"
d3	2.25"
d4	5.7"

h1	6.5"
h2	4.5"
h3	4.5"
h4	6.5"

L=35.2" (894mm) H=18.6" (472mm)

Figure 12. Geometry of the proposed triple-friction-pendulum isolator for the SGIA terminal building

Analysis procedures

In this section, a review of the analysis methods used in the performance-based design of SGIA is given. Results obtained from each analysis procedure are compared to verify the overall results. The following procedures are employed:

- Equivalent lateral force procedure
- Response spectrum procedure
- Nonlinear time-history procedure

Equivalent Lateral Force Procedure

The equivalent lateral force procedure of ASCE 7-05, Section 17.5 is permitted to be used for the design of a seismically isolated structure under the conditions explained in Section 17.4.1. This method can estimate the total base shear and maximum isolator displacements efficiently. The isolator backbone curve used in the equivalent static force procedure and the related parameters are shown in Figure 13.

Isolator displacements can be estimated by the iterative procedure defined below

Step-1:

$$D_{\mathrm{Y}} = (u_2 - u_1) R_1 \tag{12}$$

Step-2: Select an initial isolator displacement, D_{D}.

Step-3:

$$F_{\mathrm{D}} = \left[u_2 + \frac{D_{\mathrm{D}} - D_{\mathrm{Y}}}{R_2} \right] W \tag{13}$$

Step-4: Minimum effective stiffness k_{D}, ASCE Eq. (17.8-6)

$$k_{\mathrm{D}} = \frac{F_{\mathrm{D}}}{D_{\mathrm{D}}} \tag{14}$$

Step-5: Effective period T_{D}, ASCE Eq. (17.5-4)

$$T_{\mathrm{D}} = 2\pi \sqrt{\frac{W}{k_{\mathrm{D}}\, g}} \tag{15}$$

Step-6: Effective damping β_{D}, ASCE Eq. (17.8-8)

$$\beta_{\mathrm{D}} = \frac{\sum E_{\mathrm{D}}}{2\pi\, k_{\mathrm{D}}\, D_{\mathrm{D}}^2} \text{ , get } B_{\mathrm{D}} \text{ from ASCE Table 17.5-1} \tag{16}$$

Step-7: Isolator displacement D'_{D} , ASCE Eq. (17.5-3)

$$D'_{\mathrm{D}} = \frac{S_{\mathrm{D1}}\, T_{\mathrm{D}}}{4\pi^2 B_{\mathrm{D}}} \tag{17}$$

Check, if $D'_{\mathrm{D}} \approx D_{\mathrm{D}}$. Otherwise, return to Step 2

Step-8: Resultant base shear, V_{D}, ASCE Eq. (17.5-8)

$$V_{\mathrm{D}} = \frac{S_{\mathrm{D1}}}{B_{\mathrm{D}}\, T_{\mathrm{D}}} \tag{18}$$

where S_{D1} is the design 5% damped spectral acceleration parameter at 1 sec period in units of g-s.

The equivalent lateral force procedure is performed for the upper and lower isolator parameters shown in Table 2. The results of the analysis and the sensitivity of the results to a change in isolator properties are summarized at Table 3.

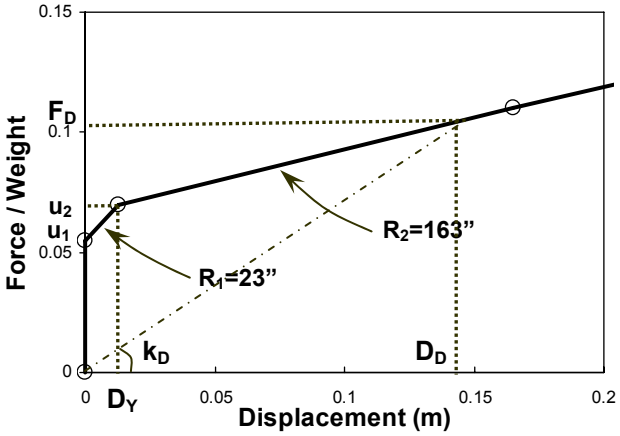

Figure 13. Isolator backbone curve for the equivalent lateral force procedure

Table 2. Upper and lower bound friction, stiffness and damping properties at DBE and MCE events

	DBE		MCE	
	Lower B	Upper B	Lower B	Upper B
u_1	0.060	0.075	0.065	0.080
u_2	0.054	0.068	0.059	0.072
u_3	0.054	0.068	0.059	0.072
u_4	0.060	0.075	0.065	0.080
K_{eff} (kN/m)	2,900	3,630	2,503	2,871
β_{eff} (%)	38%	38%	30%	30%

Table 3. Summary of the equivalent lateral force procedure results

	DBE		MCE	
	Lower B	Upper B	Lower B	Upper B
Isolator Disp. (mm)	139	110	297	235
Force/ Weight	0.093	0.103	0.137	0.140

Response Spectrum Procedure

The guidelines given by Article 4.5 of the AASHTO Standard Specification are used for the linear dynamic response spectrum analysis of the isolated SGIA building with the following modifications.

- The isolation bearings are modeled by the use of their effective stiffness, K_{eff}, which is determined at the design displacement.
- The ground response spectrum is modified to incorporate the effective damping, β_{eff}, of the isolated structure.

In order to obtain a response spectrum for a damping ratio that is different than the damping of the original response spectrum curve, the equation Eq.1-13 of ASCE 41-06 can be used:

$$B = 4/[5.6 - \ln(100\,\beta_{\text{eff}})] \qquad (19)$$

where, β_{eff} is the effective damping coefficient and, B is the scale factor that will be multiplied with the response spectrum values of a 5% damping curve. The scale factors for SGIA are estimated to be 2.04 for DBE (38%) and 1.82 for MCE (30%) event. The modified portion of the response spectrum should only be used for the isolated modes. In other words, scaling factor B is only applied to the portion of the response spectrum curve with periods greater than $0.8T_{\text{eff}}$. The response spectrum curve with 5% damping is used for all other modes. The final response spectrum curve that is used for the isolated structure is often called composite spectra and will have a form as shown in Figure 14. The modal Ritz analysis of the SGIA building shows that first two modes are isolator modes in principal directions with a total mass participation ratio of 98% each. This shows a perfect decoupling of the superstructure from the base through the isolation layer.

The summary of the results from the response spectrum procedure that are averaged over the values obtained from principle directions are shown in Table 4. Also shown is the sensitivity of the response to changes in isolator properties, which refers to the friction values obtained from the production test results. The first cycle friction is utilized to obtain the upper bound values of friction, and average 3-cycle friction is used as the lower bound friction. It is observed that upper bound isolator properties result in a decrease up to 20% in the isolator displacements and, similar to the previous analysis, approximately 5% increase in the member forces.

It is observed from the results presented in Figures 15 and 16 that equivalent lateral force and response spectrum procedures result in almost identical isolator displacement demands and base shear coefficients (these results verify the accuracy of the analysis methods). The story shear distribution is extracted, and results are presented in Figure 15. Also, floor absolute displacements, calculated by averaging point displacements of each floor, and the results are shown in Figure 16. The maximum isolator displacement demand is found to be 302 mm (= 316 − 14) in the longitudinal direction and 290 mm (= 310 − 11) in the transverse direction for the MCE hazard.

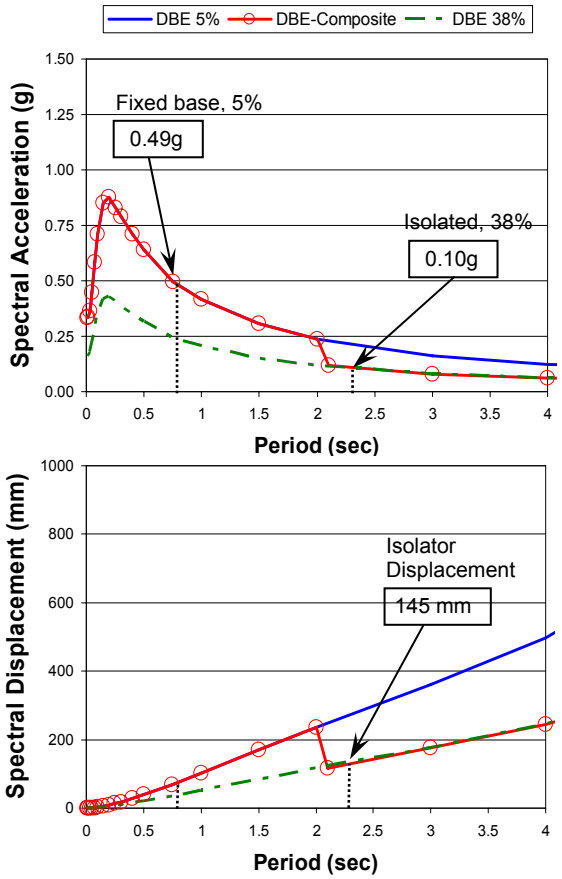

Figure 14. Composite response spectra for the DBE hazard (AASHTO, 2000)

Table 4. Summary of the results from the response spectrum procedure (averaged on directions)

	DBE		MCE	
	Lower B	Upper B	Lower B	Upper B
Isolator Disp. (mm)	145	115	296	234
Force/ Weight	0.098	0.101	0.139	0.145

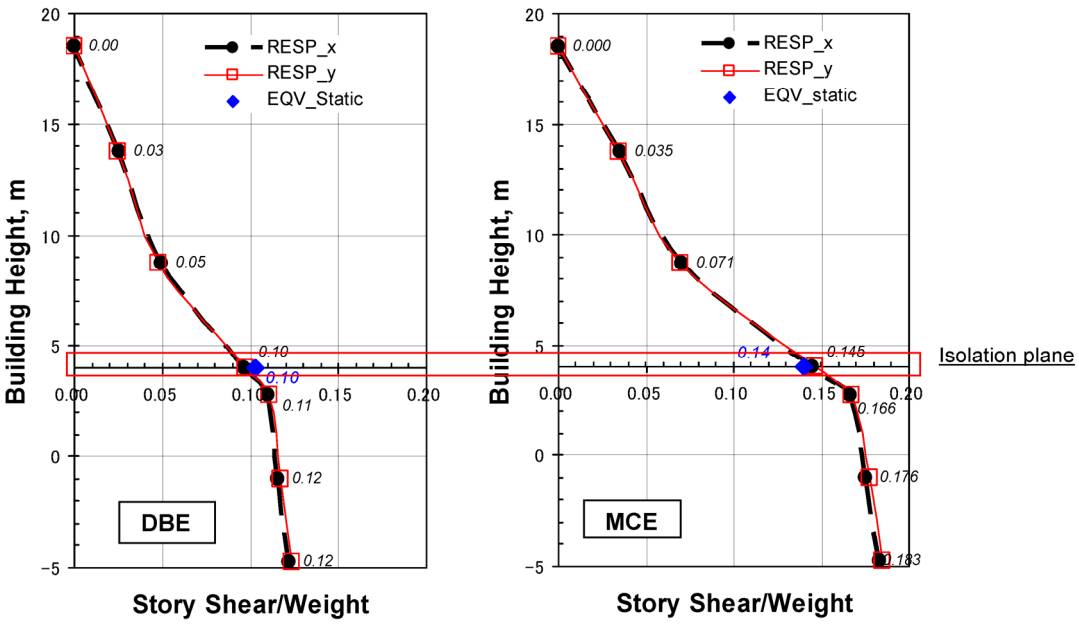

Figure 15. Story shear distribution from response spectrum analysis (upper bound) and comparison of base shear values with equivalent lateral force procedure for DBE and MCE hazards

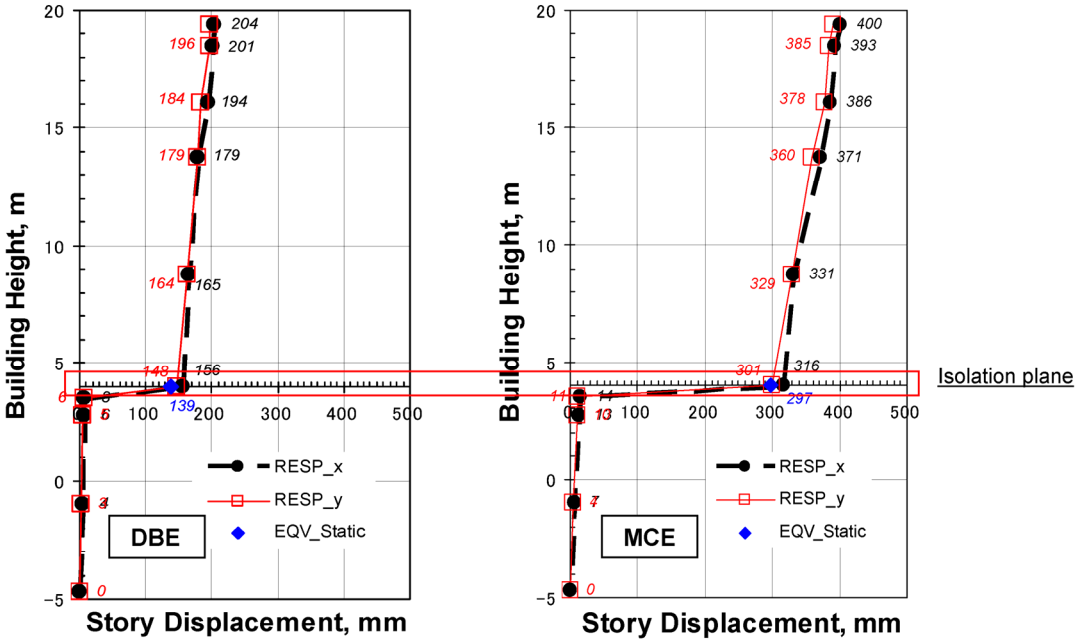

Figure 16. Story displacement from response spectrum analysis (lower bound) and comparison of isolator displacement with equivalent lateral force procedure for DBE and MCE hazards

Nonlinear Time History Procedure

In the design of the SGIA building, nonlinear time-history procedure is used for the estimation of structural responses such as maximum isolator displacements and shears as well as for the structural member performance evaluation and stability check of the system for MCE hazard. In this section, analytical modeling of isolators, seismic excitation used in the analysis and implementation of isolator nonlinearity are explained and results of the study are presented.

a) Isolator modeling:

In the linear procedures (equivalent lateral and response spectrum methods), effective stiffness (K_{eff}) and damping (β_{eff}) are the only isolator parameter used in the analysis. In the case of nonlinear time-history analysis, a new set of parameters is necessary to realize the nonlinear hysteretic behavior of the triple-friction-pendulum devices.

Herein, a Parallel Discrete Spring Model (PDSM), which has three types of nonlinear elements that are connected in parallel, is adopted for the nonlinear modeling of the isolator (Figure 17). These elements are shown in Figure 18 and summarized as follows:

1. Hysteretic Element: This element simulates the lateral stiffness and energy dissipation of the isolators. In SAP2000, this element is further modeled as two nonlinear springs that are connected parallel, which is explained in detail in the following sections.
2. Gap Element: This element simulates the vertical stiffness (compression) and resistance to the uplift (no resistance) by the isolators.
3. Hook Element: This element simulates the boundary conditions (stopper) under the ultimate horizontal displacement limits of isolators.

b) Seismic input:

As for the seismic demand, per ASCE 7-05, time history analysis shall be performed with at least three appropriate pairs of horizontal time history components. If three time history analyses are performed, the maximum response of the parameter of interest should be used for design. If seven or more time history analyses are performed, the average value of the response parameter of interest should be used for design.

Seven ground motion records from three earthquakes were selected based on matching the seismo-tectonic factors controlling the region (mechanism: strike-slip, Mw: 6.5-7.5, near field records).

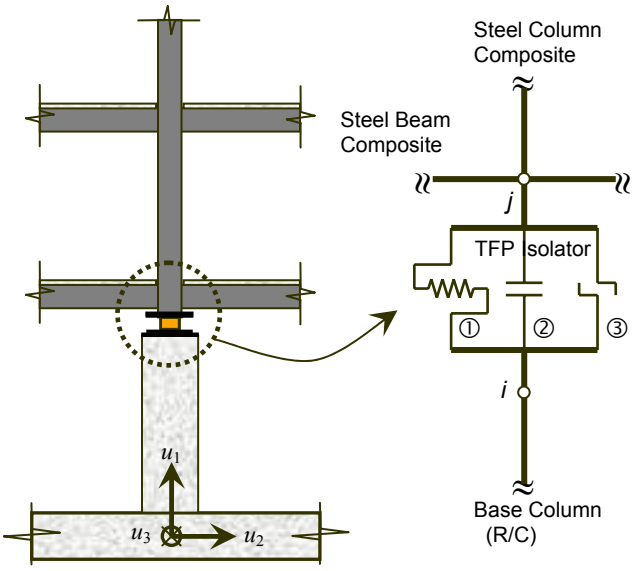

Figure 17. Nonlinear parallel discrete spring model for the triple-friction-pendulum isolators

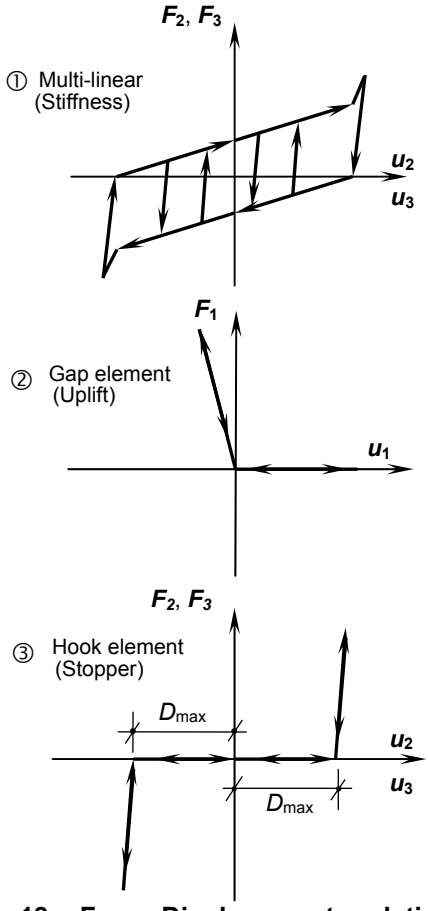

Figure 18. Force-Displacement relationships of isolator springs used in the nonlinear analysis

The selected ground motion time histories are modified to fit the amplified MCE and DBE target 5% damped acceleration spectra, considering the criteria given in ASCE 7-05 such that the SRSS spectrum of each record is not less than 90% of the amplified spectrum multiplied by 1.3 in the period range of interest (1.25 sec – 3.5 sec). Each pair of record components is applied simultaneously to the model. Then the maximum displacement of the isolation system was calculated from the vector sum of the orthogonal displacement at each time step. This analysis has repeated by switching the components in principle directions.

c) Hysteretic Element Modeling

The hysteretic element in PDSM can not be adequately captured in SAP2000 analysis. Also, user-defined multi-linear curves cannot be used since this approach will ignore the bi-directional interaction (softening) effects of the isolators. Therefore, an alternative approach is implemented in the nonlinear time history analysis. Two rubber bearings are connected in parallel to explicitly model the hysteretic element, where the first bearing element is an elastoplastic spring which represents the first pendulum friction u_1 and the modeling parameters for this element is given by

$$k_1 = 100{,}0000 \text{ (Large number)} \quad (20)$$

$$F_y = u_1 W \quad (21)$$

$$\alpha_1 = 0.00001 \text{ (Small number)} \quad (22)$$

The second rubber bearing element has an initial stiffness W/R_1, a yield force of $(u_2 - u_1)W$ and a post stiffness of W/R_2. These are summarized as

$$k_1 = W / R_1 \quad (23)$$

$$k_2 = W / R_2 \quad (24)$$

$$F_y = (u_1 - u_2)\, W \quad (25)$$

$$\alpha_2 = k_2 / k_1 \quad (26)$$

This model is called equivalent triple-friction-pendulum model in this paper. The parameters of the pendulum devices used in the SGIA building are u_1 = 5.9%, u_2 = 6.4%, R_1 = 23 in and R_2 = 167 in. Figure 19 compares the equivalent triple-friction-pendulum behavior to the target nonlinear envelope. Clearly, the alternative model provides an accurate estimate of the actual behavior from a practical design perspective.

d) Results:

The analysis performed for seven pairs of record with switching the directional components. Figure 20 shows the isolator displacement paths obtained from the different time history pairs at MCE event for a selected link couple.

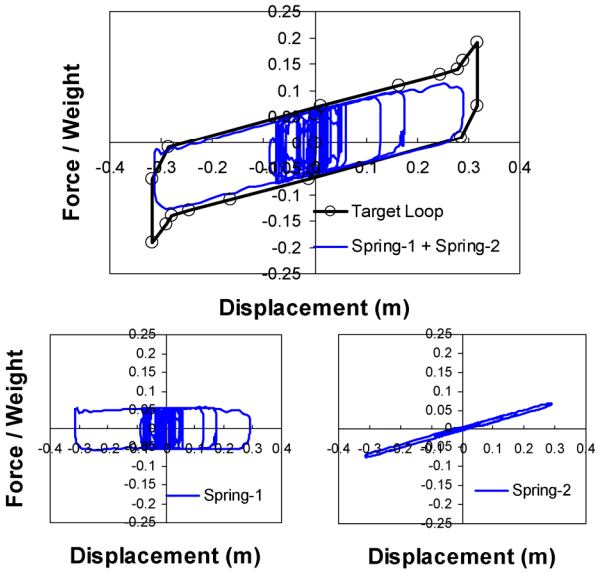

Figure 19. Hysteretic element modeling

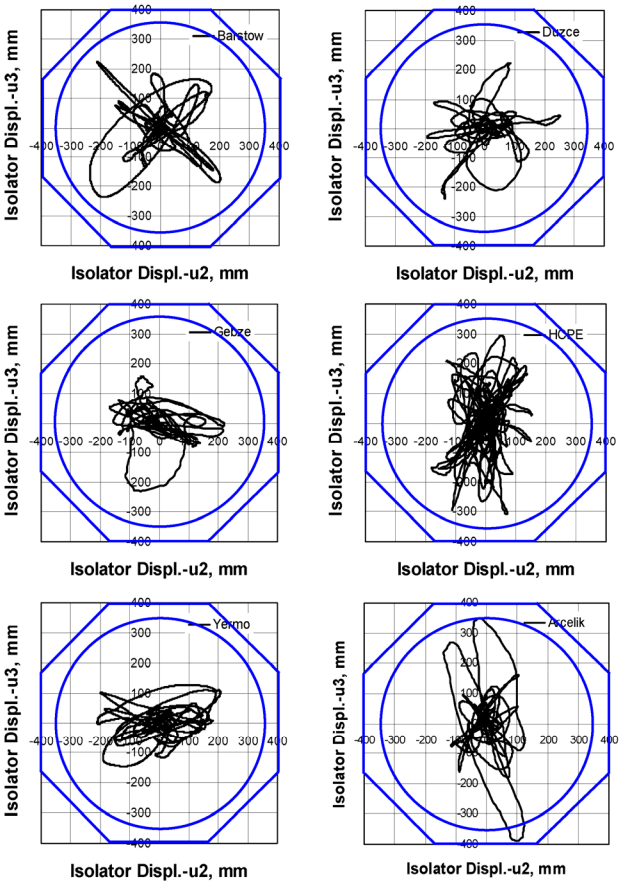

Figure 20. Isolator displacement paths obtained by time history analysis at MCE events (Link#174-56)

As can be seen in the displacement paths of Figure 20 and the summary in Table 5, the average displacement is well within the isolator capacity. In the entire record set, only one case produced a displacement in excess of the capacity. For this case a special analysis was performed to verify the integrity of the superstructure.

The nonlinear time history procedure results for the principle directions are shown in Table 5. It is observed that base shear and isolator displacements are slightly smaller than the values obtained from the equivalent lateral force and response spectrum procedures. The maximum isolator displacement demand is found to be 274 mm (= 306 − 32) in the longitudinal direction and 259 mm (= 289 − 30) in the transverse direction for the MCE hazard.

Comparing the results of the analysis of base isolated model to the fixed-base model (*i.e.*, isolator elements are replaced with fixed supports), significant decrease in the story-drift and accelerations are observed (Figure 21). Average ratio of the fixed-base building story drift to the isolated building story drift is in the order of 6. Maximum story drift at the top story of the fixed- base structure is reduced from 2% to 0.3% at the MCE level for the Barstow earthquake data. The decrease in the maximum story acceleration is even more significant, with a fixed-base to isolated model ratio of more than 10 (Figure 22). With the introduction of the base isolation, the acceleration at the building top decreased from 2*g* to 0.2*g* in average. Clearly, reduced accelerations provide significant reduction in the seismic design forces and hence, reduce the risk of structural and non-structural earthquake damage. Also, cost-savings are achieved by reducing the amount of structural steel and concrete used. It is reasonable to draw the conclusion that non-structural component damage in the fixed-base scheme would require total replacement of these elements in the case of the MCE event. In contrast, non-structural component damage and disruption to the occupancy are minimized in the isolated building. Due to the reduced inter-story drift values in the base isolated scheme, there is an opportunity for simplified envelope detailing as well. Maximum averaged story shear distributions and their minimum and maximum envelopes obtained from the time-history analysis are plotted in Figure 23 (a). Comparison to the equivalent lateral and response spectrum analysis results are also presented; at the isolation level, they show close correlation. The base-shear obtained from the time history procedure is slightly smaller than the shear obtained from the other procedures. It is also worth mentioning that, even though the averaged values (over the records and principal directions) are in good correlation with the response spectrum results, there is a significant difference between the minimum and maximum envelope. Maximum story shear distributions in transverse direction from individual record pairs are shown at Figure 23 (b).

Table 5. Summary of the results from the time history procedure (averaged on directions)

	DBE		MCE	
	Lower B	Upper B	Lower B	Upper B
Isolator Disp. (mm)	130	104	267	211
Force/ Weight	0.095	0.091	0.135	0.130

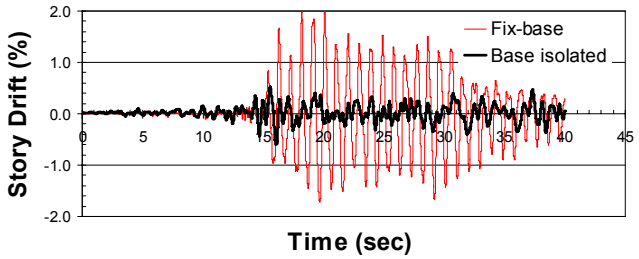

Figure 21. Comparison of top-story drift from fixed-base and base-isolated models (Barstow)

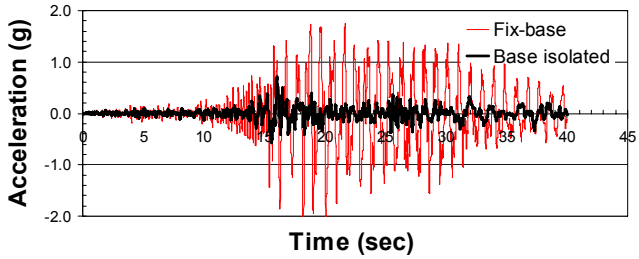

Figure 22. Comparison of top story accelerations from fixed-base and base-isolated models (Barstow)

Maximum averaged story displacements from the time history analysis together with minimum and maximum envelope are plotted in Figure 24 (a). Averaged values also show very good correlation with the results obtained from the other procedures. Again, similar to story shear, significant deviation among the story displacement results (from individual records) are observed as shown in Figure 24 (b).

The results presented show the importance of hazard studies, selection of records, and number of records used in the analysis; analysis results, design, and structural performance may vary significantly. It is believed that current code provisions for the seismically isolated buildings are not specific in this issue.

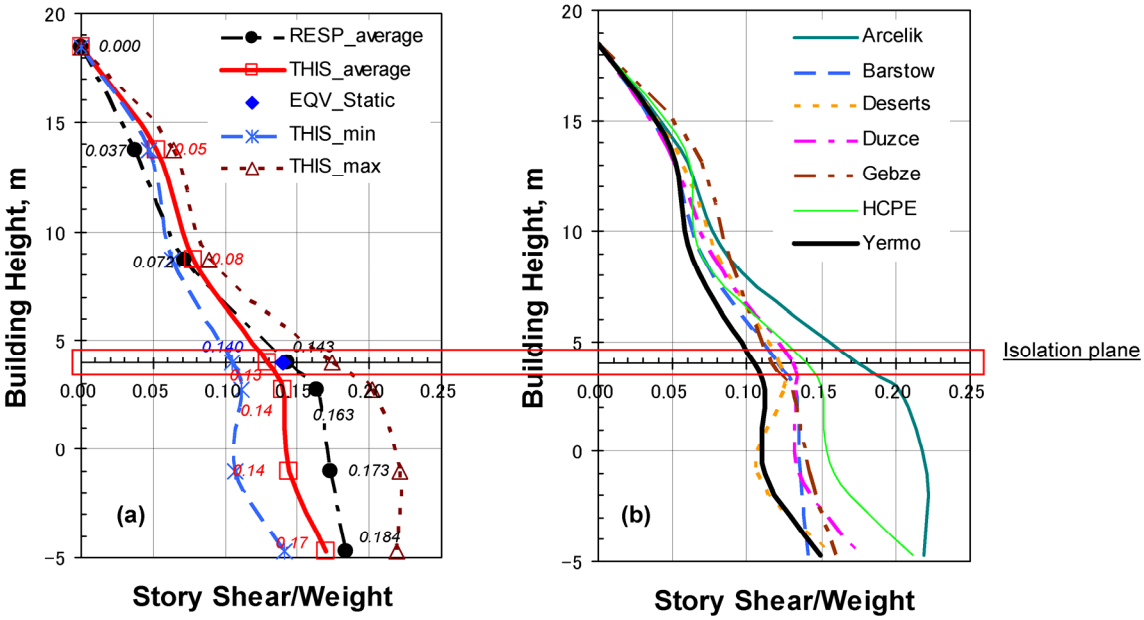

Figure 23. (a) Maximum story shear distribution from the time history analysis and comparison at MCE event, (b) Maximum story shear distribution in transverse direction by the individual record pairs

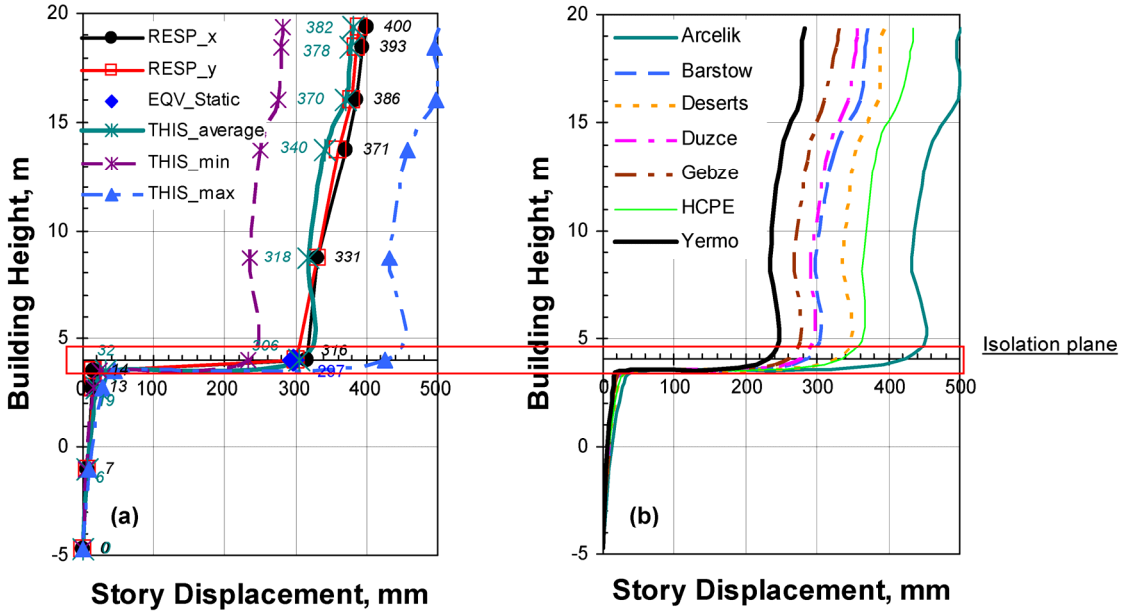

Figure 24. (a) Maximum story displacement obtained from the time history analysis and comparison at MCE event (Isolator D_{max} = 289 − 30 = 259 mm, D_{max} = 306 − 32 = 274 mm), (b) Maximum story displacements in transverse direction by the individual record pairs

Structural Performance

In this study, time history and response spectrum procedures are used for the performance evaluation of members and for stability check of the system (particularly for the MCE event). Building performance is quantified in terms of story drift and member-based demand capacity ratios at each DBE and MCE events. Nonlinear acceptance criteria for structural components defined by FEMA 356 and ASCE/SEI 41-06 are implemented. Initially, nonlinearity is assumed to be limited to the isolators (*i.e.*, the superstructure is kept elastic). When the results indicate a demand over capacity larger than the elastic limit, a nonlinear link element is assigned for those members. If the member performance does not meet the acceptance criteria, the section is modified. Analysis is then repeated until all members fulfill the expected behavior and satisfy the performance criteria.

Accidental torsion effects are included in the analysis and performance evaluation of the SGIA building, to take into account possible displacement of floor center of masses and possible differences in the distribution of lateral rigidities from their assumed locations. For a base-isolated building, ASCE 7-05 requires that accidental torsion effects should result in a minimum of 10% increase in the maximum diaphragm displacement that of an analysis without accidental torsion. Previous research has revealed that base-isolated buildings do not suffer from torsion as significantly as fixed-based buildings, and overall a 10% increase in the maximum drifts is adequate to capture these effects (Wolff and Constantinou, 2004). Overall, it is observed that accidental torsion affects did not yield a significant increase in the stress levels and ratios on most structural members. For a minor group of members (corner elements), stress increase was 30%, yet all were within the acceptable limits.

Response sensitivities due to change in the isolator properties are also included in the analysis and the performance evaluation. Upper bound properties are used in member based capacity checks and lower bound properties are employed for the deflections. It was observed that the upper bound isolator properties result in a decrease up to 20% in the isolator displacements and approximately a 5% increase in the member forces.

Maximum interstory limit from the individual records (not averaged) is less than 0.3% for DBE and 0.5% for MCE level hazard. These results can be compared with FEMA 356, Table C1.3, “Steel Moment Frames” drift limits of 0.7% for Immediate Occupancy (IO), 1% (2.5% for transient) for Life Safety (LS) and 5% for Collapse Prevention (CP).

The maximum predicted isolator displacement in the MCE level earthquake hazard is 297 mm (equivalent lateral force, response spectrum and time history procedures) which is less than the isolator allowable limit of 345 mm.

A design stress check based on AISC 1999 (LRFD) showed that the structure behaves elastically (D/C < 1) under the DBE hazard using the response spectrum and time history analysis along with the upper bound isolator properties and accidental torsion effects. Stress check for the MCE level hazard is also performed by using the response spectrum as well as time history analysis for the seven record pairs (note that this stress check is not required by ASCE 7-05). The stress check maxima results for the response spectrum and time history (not averaged) analysis are;

- Majority of the columns < 1.3
  (FEMA 356 *m*-factor for IO is 2.0)
- All Beams < 2.0
  (FEMA 356 *m*-factor for IO is 2.0)

No specific procedures exist for averaging the stress ratios of the time history results from the seven MCE pairs. However, if the maximum stress ratios from the time history analysis were scaled using average base shear of 13%, divided by maximum base shear of 16% from the individual time history analysis, it could have been easily argued that columns would be very close to their elastic limit, while beams would be expected to experience a moderate amount of inelastic behavior.

Construction Milestones

Important milestones of the SGIA terminal building construction are summarized as follows:

- The construction has started with the soil excavation and foundation pile construction in April 2008.
- The construction of the pile caps, rest of the foundation and basement retaining walls started at the end of April 2008.
- The construction of reinforced concrete columns below the isolation layer started in May 2008.
- The tender for the steel structure was held mid-June 2008 with six subcontractors.
- The placement of the triple-friction-pendulum devices started in July 2008 (Figure 25 and 26).
- In August 2008, the erection of the steel structure started (Figures 27 and 28).
- The erection of the steel roof purlin structure started in November 2008 (Figure 29, 30 and 31).
- The installation of service components (mechanical, electrical and plumbing) started in January 2009.
- Current estimated date of completion is 29 October 2009.

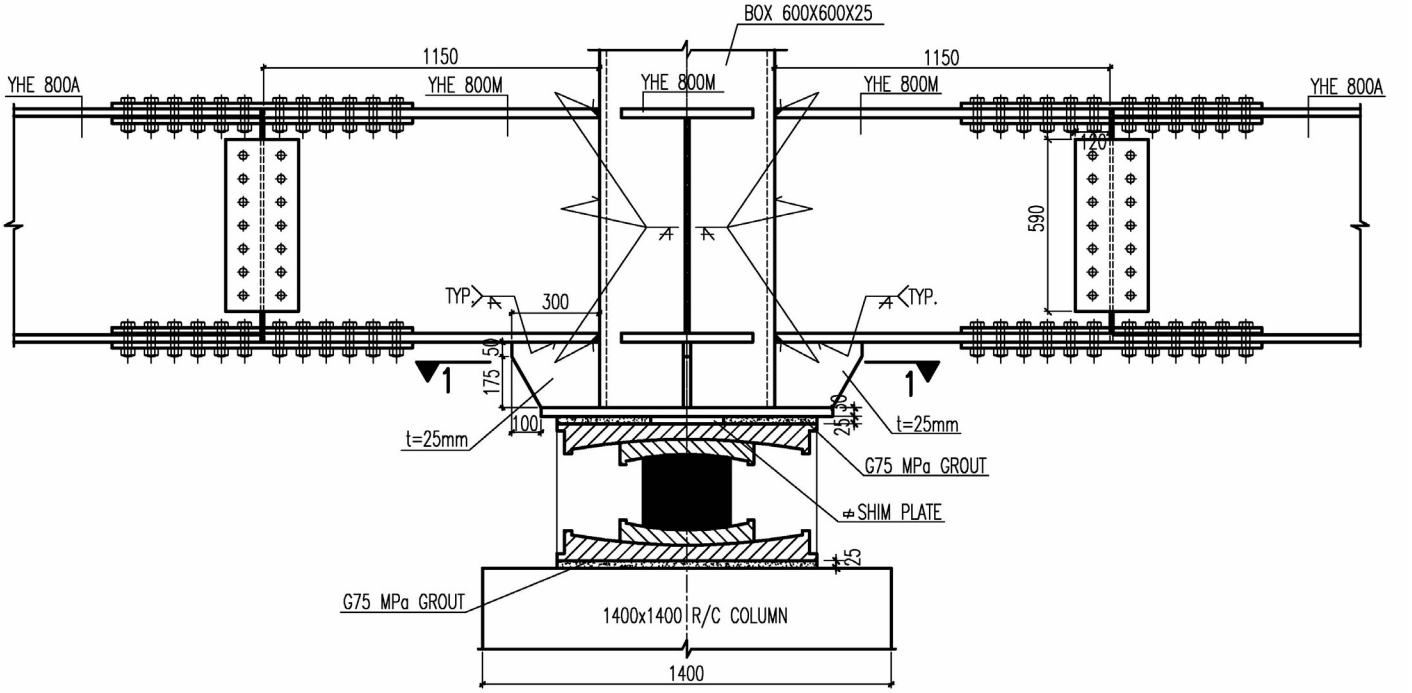

TYPICAL COLUMN–ISOLATOR CONNECTION DETAIL
1/10

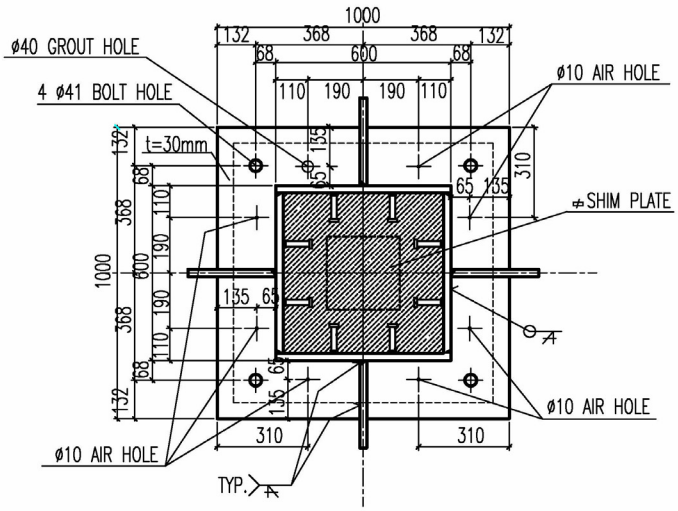

SECTION 1–1
1/10

Figure 25. Typical column to isolator connection detail

Figure 26. Placement of a typical isolator

Figure 27. Isolator-column-beam connection

Figure 28. Superstructure steel moment frame

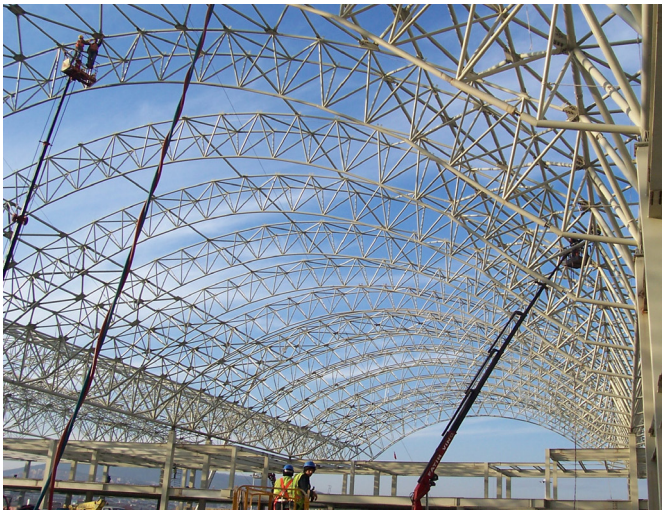

Figure 29. Placement of the roof purlin system

Figure 30. Space frame roof trusses and bracings

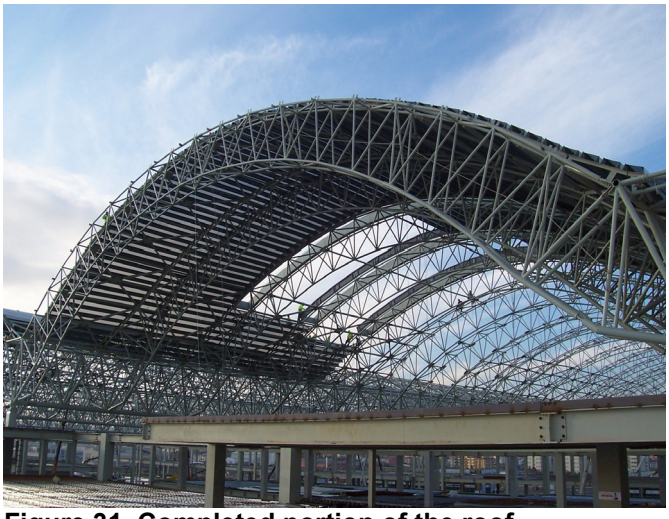

Figure 31. Completed portion of the roof

Concluding Remarks

The following conclusions are derived from the performance-based design of the SGIA terminal building:

(1) For DBE hazards, the total base shear calculated by the equivalent lateral force, response spectrum and time history methods are consistent within a value of 10% of total seismic weight (all analysis unscaled, $R = 1$).
(2) For MCE hazard level, the total base shear calculated by the equivalent lateral force method is 14%, 13% average (maximum 16%) using time history and 14% by the response spectrum methods.
(3) The equivalent lateral force typically predicts the displacement demand well or conservatively as obtained by the time history analysis results.
(4) The time history method typically predicts smaller member forces and displacements compared to the equivalent lateral force and response spectrum analysis.
(5) Although time history results that are averaged over the records on principal directions are in good correlation with the response spectrum results, there is a significant deviation between the minimum and maximum envelopes.
(6) The maximum predicted isolator displacement in the MCE scenario is 297 mm (among the three analysis procedures), which is less than the isolator allowable limit of 345 mm.
(7) Maximum inter-story drift is less than 0.3% for the DBE and 0.5% for the MCE level hazards. These results can be compared with FEMA-356 Table C1.3 "Steel Moment Frames" drift limits of 0.7% for Immediate Occupancy, 1% (2.5% for transient) for Life Safety and 5% for Collapse Prevention.
(8) Response sensitivity to change in isolator properties was also studied. It was observed that upper bound isolator properties decrease up to 20% in isolator displacements and approximately 5% increase in member forces.
(9) Accidental torsion effects are incorporated into the model. Increase in the member forces due to the accidental torsion is observed to be minimal for most of the members; for the others; these are members on the corners, the increase was within the acceptable limits.
(10) Design stress check for AISC 1999 (LRFD) showed that the structure behaves elastically (D/C < 1) under the DBE hazard using response spectrum and time history analysis along with the upper bound isolator properties and accidental torsion effects.
(11) Stress check for the MCE level hazard has also been performed by using response spectrum as well as time history analysis of seven record pairs, where the maximum of the stress ratios obtained from response spectrum and time-history analysis are

Majority of the Columns < 1.3
(FEMA 356 *m*-factor for IO is 2.0)
All Beams < 2.0
(FEMA 356 *m*-factor for IO is 2.0)

No specific procedures exist for averaging stress ratios of time history results from the seven MCE pairs. However, if the maximum stress ratios from the time-history analysis were scaled using the average base shear of 13%, divided by the maximum base shear of 16% from the individual time history analysis, it could have been easily argued that columns would be near the elastic limit while beams would be expected to experience moderate amount of inelastic behavior.

(12) Overall, the seismically isolated structure met and surpassed the performance objectives while achieving an 80% reduction in the base shear (relative to the fixed-base building model), significant decrease in the story drift (83%) and floor accelerations (90%).

Acknowledgements

The authors would like to acknowledge the team effort by Mr. Serdar Karahasanoglu, Mr. Cem Haydaroglu and other SGIA design team members from the Arup Istanbul office. The technical support by Mr. Stanley Low, Dr. Victor Zayas and Dr. Anoop S. Mokha from EPS is gratefully acknowledged. The authors would also like to thank to Prof. Mustafa Erdik from Bogazici University, Turkey for providing the extensive site-specific probabilistic seismic hazard study, and Prof. Michael. C. Constantinou from SUNY, Buffalo and Prof. Haluk Sucuoglu from Middle East Technical University, Turkey for peer reviewing the base isolation design. The logistic support from the constructor of SGIA terminal building, Limak is also acknowledged. Finally, authors would like to thank to Mr. Simon Rees from the Arup Los Angeles office for his review of this paper.

References

AASHTO, 2000, *Guide Specifications for Seismic Isolation Design (Interim), American Association of State Highway and Transportation Officials*, Washington, District of Columbia.

AISC, 1999, *Steel Construction Manual*, *American Institute of Steel Construction*, Chicago, Illinois.

ASCE, 2005, *Minimum Design Loads for Buildings and Other Structures* (*ASCE 7-05*), *American Society of Civil Engineers*, Reston, Virginia.

ASCE, 2006, *Seismic Rehabilitation of Existing Buildings* (*ASCE 41-06*), *American Society of Civil Engineers*, Reston, Virginia.

Belirti, 2008, "Sabiha Gökçen International Airport Terminal Building Geotechnical Measurements, (in Turkish)" *Belirti Mühendislik-Danişmanlik Inc.*, Istanbul, Turkey.

Boore, D.M., and Atkinson G. M., 2008, "Ground-Motion Prediction Equations for the Average Horizontal Component of PGA, PGV, and 5%-Damped PSA at Spectral Periods between 0.01 s and 10.0 s" *Earthquake Spectra,* Vol. 24, No. 1, p 99–138.

Campbell, K. W. and Y. Bozorgnia, 2008, "NGA Ground Motion Model for the Geometric Mean Horizontal Component of PGA, PGV, PGD and 5% Damped Linear Elastic Response Spectra for Periods Ranging from 0.01 to 10 s" *Earthquake Spectra,* Vol. 24, No. 1, p 139–171.

Erdik, M., Sesetyan, K., Demircioglu, M. B., and Durukal, E., 2008, "Assesment of Site-Specific Earthquake Hazard for the New International Terminal of Sabiha Gökçen Airport (Internal Report)," *Bogazici University*, Istanbul, Turkey.

FEMA, 2000, *Prestandard and commentary for the seismic rehabilitation of buildings* (*FEMA 356*), *Federal Emergency Management Agency*, Washington, District of Columbia.

Fenz, D.M., and Constantinou, M.C., 2008a, "Modeling Triple Friction Pendulum Bearings for Response History Analysis," *Earthquake Spectra*, Vol. 24, No. 4, p 1011-1028.

Fenz, D.M., and Constantinou, M.C., 2008b, "Mechanical behavior of Multi-Spherical Sliding Bearings, Report No. MCEER-08-0007," *Multidisciplinary Center for Earthquake Engineering Research*, Buffalo, New York.

GMR, 2008, "GMR Consortium's Turkish Venture Takes Off," *Press Release*.

ICBO, 2006, International Building Code (IBC 2006), *International Code Council*, Country Club Hills, Illinois.

NEHRP, 2003, *NEHRP Recommended Provisions for Seismic Regulations for New Buildings and Other Structures Part 1: Provisions (FEMA 450)*, *Building Seismic Safety Council*, Washington, District of Columbia.

TEC, 2007, *Specifications for Structures to be Built in Disaster Areas* (*TEC 98/07*)," *Ministry of Public Works and Resettlement*, Ankara, Turkey.

USGS, 2000, "Implications for Earthquake Risk Reduction in the United States from the Kocaeli, Turkey, Earthquake on August 17, 1999, Circular 1193," *United States Geological Survey*, Denver, Colorado.

Wolff, E. D., and Constantinou M. C., 2004, "Experimental Study of Seismic Isolation Systems with Emphasis on Secondary System Response and Verification of Accuracy of Dynamic Response History Analysis Methods, Report No. MCEER-04-0001," *Multidiciplinary Center for Earthquake Engineering Research*, Buffalo, New York.

Zayas, V., Low, S., and Mokha A., 2008a, "Design of the Seismic Isolation System and Prototype Test Results for the FPT4600/14/3/31 Triple Pendulum Bearings for the New Sabiha Gökçen International Terminal Building, Istanbul, Turkey (Internal Report)," *Earthquake Protection Systems*, Vallejo, California.

Zayas, V., Low, S., and Mokha A., 2008b, "ASCE 7-05 Prototype Bearing Test Report for the FPT4600/14/3/31 Triple Pendulum Bearings for the New Sabiha Gökçen International Terminal Building, Istanbul, Turkey (Internal Report)," *Earthquake Protection Systems*, Vallejo, California.

Zayas, V., Low, S., and Mokha A., 2008c, "Production Triple Pendulum Bearing Quality Control Test Report Submittal for Bearing Type FPT4600/14/3/31, Bearing No. 1 to 76 for the New Sabiha Gökçen International Terminal Building, Istanbul, Turkey (Internal Report)," *Earthquake Protection Systems*, Vallejo, California.